



---

*Research article*

## Fixed-time consensus control of stochastic nonlinear multi-agent systems with input saturation using command-filtered backstepping

Yifan Liu, Guozeng Cui\* and Ze Li

School of Electronic and Information Engineering, Suzhou University of Science and Technology, Suzhou 215009, China

\* **Correspondence:** Email: [guozengcui@gmail.com](mailto:guozengcui@gmail.com).

**Abstract:** In this paper, a fixed-time consensus control algorithm is proposed for non-triangular structure stochastic nonlinear multi-agent systems (SNMASs) with input saturation via the command-filtered backstepping design method. Fuzzy logic systems are employed to identify the nonlinear dynamics of each agent. By introducing the fixed-time command filter and constructing the fractional power error compensation mechanism, the “complexity explosion” problem is effectively avoided, and the influence of filtered errors is eliminated in a fixed time. Based on the fixed-time stability theory, it strictly proves that all signals in the closed-loop system are fixed-time bounded in probability, and the consensus error converges to a sufficiently small neighborhood of the origin in probability within a fixed time. Finally, a comparison simulation example verifies the effectiveness and superiority of the proposed fixed-time consensus control strategy.

**Keywords:** fuzzy logic system; fixed-time control; consensus control; command-filtered backstepping; SNMASs

**Mathematics Subject Classification:** 93B52, 93C42

---

### 1. Introduction

Multi-agent systems (MASs) possess autonomous perception, decision-making, and action implementation capabilities, and these agents execute intricate control tasks through communication and cooperation collectively [1]. Owing to their distinctive collaboration abilities, MASs have shown significant potential applications in various areas, including formation control of unmanned aerial vehicles [2, 3], coordinated control of multiple robotic arms [4], and synchronization control of distributed spacecraft [5]. Given the prevalence of stochastic disturbances in engineering and most actual control systems being nonlinear, many scholars are increasingly drawn to the control problems of stochastic nonlinear multi-agent systems (SNMASs) [6–8]. The stochastic disturbances

significantly complicate the control system design process, and the effective distributed control algorithm for SNMASs has become both critical and challenging.

By employing the backstepping design method, a distributed adaptive containment control scheme was presented for strict-feedback SNMASs [9]. Considering that the states of SNMASs are unmeasurable, a distributed adaptive output-feedback control algorithm was devised in [10]. Nevertheless, the “complexity explosion” problem arises in classic backstepping-based distributed control strategies. In [11], an event-triggered distributed containment control strategy was developed by applying the dynamic surface control method, effectively avoiding the “complexity explosion” problem. However, it should be noted that [11] does not consider the impact of filtered errors on system performance. Moreover, the distributed control schemes [9–11] are only applicable to strict-feedback SNMASs and cannot be extended to more general SNMASs in non-triangular form. For non-triangular structure SNMASs, the nonlinear terms involve all state variables of each agent, and directly employing the aforementioned distributed control algorithms may lead to the algebraic loop problem.

Based on the command filter technique combined with state observers, the distributed output-feedback control problem was studied for non-triangular structure SNMASs with unmeasurable states [12, 13]. Considering non-triangular structure SNMASs are subject to unknown control gains and output constraints, a command-filter-based distributed consensus algorithm was proposed in [14]. By adopting the command filter technique, these distributed algorithms [12–14] address the “complexity explosion” problem and remove the impact of filtered errors. Nonetheless, they can only ensure the asymptotic convergence of SNMASs. Subsequently, a finite-time distributed control strategy was presented for SNMASs with sensor faults [15]. In [16], the finite-time optimized control for SNMASs with non-triangular structure and non-affine nonlinear faults was investigated. It should be pointed out that the convergence time of finite-time distributed control strategies is closely tied to the system’s initial states, and the control strategies may become ineffective when these initial states are difficult to obtain or even unattainable. In [17], a fixed-time control theory was put forward, and the upper bound of the system’s convergence time is unaffected by the initial states, which are related to the controller’s parameters. Considering non-triangular structure SNMASs with actuator faults, the fixed-time distributed fault-tolerant control issue was addressed in [18]. To lessen the communication burden of non-triangular structure SNMASs, an event-trigger-based fixed-time containment control algorithm was formulated [19]. In [20], the event-triggered fixed-time containment control algorithm for SNMASs with input-delay was presented.

Note that SNMASs are prone to input saturation due to actuator constraints imposed by mechanical structures or component performance. While collaboration among multi-agent systems heavily relies on continuous and accurate control inputs, ignoring input saturation may directly impact the system’s coordination capabilities. Thus, it is necessary to properly address the SNMASs with input saturation. Considering state-constrained SNMASs with input saturation, by designing the saturation controller to avoid the input limitation problem, a distributed event-triggered control scheme was proposed in [21]. By constructing compensation systems, the issues of finite-time control and prescribed performance control for SNMASs with input saturation were investigated in [22, 23], respectively. For SNMASs with input saturation and sensor faults, an adaptive fault-tolerant containment control strategy was designed in [24], where the saturation function was approximated by a smooth function. By far, there are few results available on the fixed-time distributed control of non-triangular structure SNMASs with

an input saturation based on command-filtered backstepping design approach.

Inspired by the preceding discussions, for non-triangular structure SNMASs with input saturation, this paper presents a fixed-time consensus control algorithm based on the command-filtered backstepping design method. Compared to existing results, the main contributions of this paper are given as follows:

(1) Unlike the backstepping control schemes [9, 10] and the dynamic surface control strategies [11] for strict-feedback SNMASs, this paper targets the more general non-triangular structure SNMASs. By constructing a fixed-time command filter and a fractional power error compensation mechanism, the proposed fixed-time distributed consensus control algorithm not only addresses the “complexity explosion” problem but also removes the impact of filtered errors on the performance of SNMASs in a fixed time.

(2) Different from the asymptotic convergence control schemes [12–14] and finite-time convergence control schemes [15, 16] for non-triangular structure SNMASs, this paper proposes a fixed-time distributed consensus control scheme, whose upper bound of convergence time is not influenced by the initial states of each agent. By adjusting control parameters, it ensures that the consensus error converges to a sufficiently small neighborhood of the origin in probability within a fixed time.

(3) Compared with conventional approaches for anti-saturation algorithms [22, 23], this paper designs a compensation system with fixed-time convergence that resolves the limitation of input saturation.

## 2. Problem formulation and preliminaries

### 2.1. Graph theory

To denote the communication relations among  $N$  followers in SNMASs, a directed graph

$$\mathfrak{N}_G = (\mathcal{V}_G, \mathcal{E}_G)$$

is employed, with  $\mathcal{E}_G \subseteq \mathcal{V}_G \times \mathcal{V}_G$  denoting the edge set and  $\mathcal{V}_G = \{1, \dots, N\}$  being the node set.

$$\mathfrak{N}_m = \{l \mid (l, m) \in \mathcal{E}_G\}$$

is defined as the neighbors set for node  $m$ , where the directed edge  $(l, m) \in \mathcal{E}_G$  denotes that the  $m$ -th follower can acquire information from the  $l$ -th follower. The adjacency matrix

$$\mathfrak{C}_G = [c_{m,l}] \in \mathbf{R}^{N \times N}$$

is defined as  $c_{m,l} = 1$  if  $(l, m) \in \mathcal{E}_G$  and  $c_{m,l} = 0$  if  $(l, m) \notin \mathcal{E}_G$ . The Laplacian matrix is represented as

$$\mathfrak{B}_G = \mathfrak{J}_G - \mathfrak{C}_G,$$

in which

$$\mathfrak{J}_G = \text{diag}\{J_1, \dots, J_N\}, \quad J_m = \sum_{l=1}^N c_{m,l}.$$

Furthermore, an augmented directed graph

$$\bar{\mathfrak{N}}_G = (\bar{\mathcal{V}}_G, \bar{\mathcal{E}}_G)$$

is applied to describe the communication relations between the leader 0 and the  $N$  followers.

$$\mathfrak{L}_G = \text{diag} \{ \ell_1, \dots, \ell_N \}$$

in which  $\ell_m = 1$ , if the  $m$ -th follower can acquire information from the leader, otherwise  $\ell_m = 0$ . If there exists at least one directed path from the leader to other followers, then the augmented graph contains a directed spanning tree.

## 2.2. Stochastic theory

Consider the following stochastic nonlinear system:

$$d\zeta = q(\zeta)dt + p(\zeta)d\omega, \quad (2.1)$$

where  $\zeta$  stands for the state vector;  $q(\zeta)$  and  $p(\zeta)$  are smooth nonlinear functions satisfying  $q(0) = 0$  and  $p(0) = 0$ .  $\omega$  represents an  $s$ -dimensional independent standard Brownian motion.

**Definition 1.** [25] For any continuous positive-definite Lyapunov function  $V(\zeta) \in C^2$  associated with system (2.1), define its differential operator  $\mathcal{L}V(\zeta)$  as

$$\mathcal{L}V(\zeta) = \frac{\partial V(\zeta)}{\partial \zeta} q(\zeta) + \frac{1}{2} \text{Tr} \left\{ p^\top(\zeta) \frac{\partial^2 V(\zeta)}{\partial \zeta^2} p(\zeta) \right\}.$$

## 2.3. Problem formulation

Consider the following non-triangular SNMASs composed of one leader and  $N$  followers, where the dynamics of the  $m$ -th follower are described as

$$\begin{cases} dx_{m,b} = (x_{m,b+1} + f_{m,b}(x_m)) dt + h_{m,b}^\top(x_m) d\omega, \\ dx_{m,n_m} = (u_m(\varphi_m) + f_{m,n_m}(x_m)) dt + h_{m,n_m}^\top(x_m) d\omega, \\ y_m = x_{m,1}, \end{cases} \quad (2.2)$$

where  $m = 1, \dots, N$ ,  $b = 1, \dots, n_m - 1$ ;

$$x_m = [x_{m,1}, \dots, x_{m,n_m}]^\top \in \mathbf{R}^{n_m}$$

represents the state vector;  $y_m \in \mathbf{R}$  is the output signal of the  $m$ -th follower.

$$f_{m,b}(\cdot) : \mathbf{R}^{n_m} \mapsto \mathbf{R} \quad \text{and} \quad h_{m,b}(\cdot) : \mathbf{R}^{n_m} \mapsto \mathbf{R}^s$$

are unknown smooth nonlinear functions.  $u_m(\varphi_m)$  is the system input affected by saturation nonlinearity with

$$u_m(\varphi_m) = \begin{cases} u_{m,\max}, & \varphi_m \geq u_{m,\max}, \\ \varphi_m, & u_{m,\min} < \varphi_m < u_{m,\max}, \\ u_{m,\min}, & \varphi_m \leq u_{m,\min}, \end{cases}$$

where  $u_{m_{\max}} > 0$  and  $u_{m_{\min}} < 0$  are constants;  $\varphi_m$  is the input of saturation nonlinearity. A smooth hyperbolic tangent function  $\iota_m(\varphi_m)$  is introduced as

$$\iota_m(\varphi_m) = \begin{cases} u_{m_{\max}} * \tanh\left(\frac{\varphi_m}{u_{m_{\max}}}\right), & \varphi_m \geq 0, \\ u_{m_{\min}} * \tanh\left(\frac{\varphi_m}{u_{m_{\min}}}\right), & \varphi_m < 0, \end{cases}$$

then  $u_m(\varphi_m)$  can be rewritten as

$$u_m(\varphi_m) = \iota_m(\varphi_m) + \bar{\iota}_m(\varphi_m),$$

where

$$|\bar{\iota}_m(\varphi_m)| = |u_m(\varphi_m) - \iota_m(\varphi_m)| \leq \max\{u_{m_{\max}}(1 - \tanh(1)), u_{m_{\min}}(\tanh(1) - 1)\} = D_m.$$

**Control objective.** The aim of this paper is to develop a fixed-time distributed control scheme those ensures the outputs of all followers are synchronized with those of the leader  $r(t)$ , and the consensus error  $y_m - r(t)$  converges to a sufficiently small neighborhood of the origin in probability within a fixed time.

**Assumption 1.** The augmented graph  $\bar{\mathfrak{N}}_G$  contains a spanning tree, and  $\mathfrak{F}_G + \mathfrak{L}_G$  is invertible.

**Assumption 2.** The leader's signal  $r(t)$  is first-order continuously differentiable and bounded.

**Lemma 1.** [26,27] For a continuous function  $F(x)$  defined on a compact set  $\Omega$  and any given constant  $\varepsilon > 0$ , there exists a fuzzy logic system (FLS)  $\Phi^T(x)S(x)$  such that

$$F(x) = \Phi^T(x)S(x) + \sigma(x), \quad |\sigma(x)| \leq \varepsilon,$$

where

$$\Phi = [\phi_1(x), \dots, \phi_w(x)]^T$$

represents the ideal weight vector;

$$S(x) = [S_1(x), \dots, S_w(x)]^T / \sum_{b=1}^w S_b(x)$$

denotes the basis functions;  $w$  is the number of fuzzy rules;

$$S_b(x) = \exp\left[-(x - \varphi_b)^T(x - \varphi_b) / \tau_b^2\right],$$

where  $\varphi_b$  is the center of the Gaussian function, and  $\tau_b$  is the width.

**Lemma 2.** [28] For  $X_1, X_2 \in R$  and  $q_1, q_2, q_3 > 0$ , the following inequality holds

$$|X_1|^{q_1}|X_2|^{q_2} \leq \frac{q_1}{q_1 + q_2} q_3 |X_1|^{q_1+q_2} + \frac{q_2}{q_1 + q_2} q_3^{-\frac{q_1}{q_2}} |X_2|^{q_1+q_2}.$$

**Lemma 3.** [29] For  $\mu_b \in R$ ,  $b = 1, \dots, \varpi$ , the following inequalities hold:

$$\sum_{b=1}^{\varpi} |\mu_b|^\lambda \geq \left(\sum_{b=1}^{\varpi} |\mu_b|\right)^\lambda, \quad 0 < \lambda \leq 1,$$

$$\sum_{b=1}^{\varpi} |\mu_b|^\lambda \geq \varpi^{1-\lambda} \left(\sum_{b=1}^{\varpi} |\mu_b|\right)^\lambda, \quad \lambda > 1.$$

**Lemma 4.** [30] For the radially unbounded Lyapunov function  $V(\zeta) \in C^2$  associated with system (2.1), if  $k_{d_1} > 0$ ,  $k_{d_2} > 0$ ,  $0 < d_1 < 1$ ,  $d_2 > 1$ ,  $\eta > 0$ , satisfying

$$\mathcal{L}V(\zeta) \leq -k_{d_1} V^{d_1}(\zeta) - k_{d_2} V^{d_2}(\zeta) + \eta,$$

then (2.1) is practical fixed-time stable in probability. Furthermore, the convergence time  $T$  satisfies

$$E(T) \leq T_{\max} = \frac{1}{k_{d_1} \varsigma (1 - d_1)} + \frac{1}{k_{d_2} \varsigma (d_2 - 1)},$$

and the solution set is given by

$$\zeta \in \left\{ V(\zeta) \leq \min \left\{ \left( \frac{\eta}{(1 - \varsigma) d_1} \right)^{1/d_1}, \left( \frac{\eta}{(1 - \varsigma) d_2} \right)^{1/d_2} \right\} \right\}, \quad \varsigma \in (0, 1).$$

### 3. Main results

In this section, a fixed-time distributed control algorithm for SNMASs with input saturation is proposed. Before the command-filtered backstepping design process, define the following constants:

$$\theta_{m,b} = \|\Phi_{m,b}\|^2, \quad \theta_m = \max \{\theta_{m,1}, \theta_{m,2}, \dots, \theta_{m,n_m}\},$$

in which  $m = 1, \dots, N$ ,  $b = 1, \dots, n_m$ .  $\hat{\theta}_{m,b}$  represents the estimated value of  $\theta_{m,b}$ , and  $\tilde{\theta}_{m,b} = \theta_{m,b} - \hat{\theta}_{m,b}$  is the estimation error.

Define the following synchronization errors for the  $m$ -th follower:

$$s_{m,1} = \sum_{l=1}^N c_{m,l} (y_m - y_l) + \ell_m (y_m - r), \quad (3.1)$$

$$s_{m,b} = x_{m,b} - \pi_{m,b}, \quad b = 2, \dots, n_m, \quad (3.2)$$

where  $\pi_{m,b}$  is the output signal of a fixed-time command filter and the distributed virtual control signal  $\alpha_{m,b}$  is the input signal. Design the fixed-time command filter as follows:

$$\begin{cases} \dot{\mu}_{m,b,1} = -\mathcal{B}_{m,b,1} \mathfrak{X}_{m,b,1}(\chi_{m,b}) + \mu_{m,b,2}, \\ \dot{\mu}_{m,b,2} = -\mathcal{B}_{m,b,2} \mathfrak{X}_{m,b,2}(\chi_{m,b}), \end{cases} \quad (3.3)$$

where  $b = 1, \dots, n_m - 1$ ,

$$\begin{aligned} \mathfrak{X}_{m,b,1}(\chi_{m,b}) &= \left( |\chi_{m,b}|^{\frac{1}{2}} + \kappa_{m,b} |\chi_{m,b}|^{\frac{3}{2}} \right) \text{sign}(\chi_{m,b}), \\ \mathfrak{X}_{m,b,2}(\chi_{m,b}) &= 2\kappa_{m,b} \chi_{m,b} + \left( \frac{1}{2} + \frac{3}{2} \kappa_{m,b}^2 |\chi_{m,b}|^2 \right) \text{sign}(\chi_{m,b}), \\ \chi_{m,b} &= \mu_{m,b,1} - \alpha_{m,b}, \quad \mu_{m,b,1} = \pi_{m,b}, \end{aligned}$$

and  $\mathcal{B}_{m,b,1} > 0$ ,  $\mathcal{B}_{m,b,2} > 0$ ,  $\kappa_{m,b} > 0$  are the filter parameters.

**Remark 1.** After introducing the fixed-time command filter (3.3), the derivative of the virtual control signal  $\alpha_{m,b}$  can be quickly approximated by the filter output signal, as a result the “complexity explosion” problem encountered in traditional backstepping approaches [9, 10] is skillfully addressed.

To eliminate the impact of filtered errors on system performance, design the error compensation signal  $\xi_{m,b}$  as follows:

$$\dot{\xi}_{m,1} = -v_{m,1}\xi_{m,1}^{4d_1-3} - k_{m,1}\xi_{m,1}^{4d_2-3} + (\ell_m + J_m)(\xi_{m,2} + \pi_{m,2} - \alpha_{m,1}), \quad (3.4)$$

$$\dot{\xi}_{m,b} = -v_{m,b}\xi_{m,b}^{4d_1-3} - k_{m,b}\xi_{m,b}^{4d_2-3} + \xi_{m,b+1} + \pi_{m,b+1} - \alpha_{m,b}, \quad (3.5)$$

$$\dot{\xi}_{m,n_m} = -v_{m,n_m}\xi_{m,n_m}^{4d_1-3} - k_{m,n_m}\xi_{m,n_m}^{4d_2-3}, \quad (3.6)$$

where  $b = 2, \dots, n_m - 1$ ,  $3/4 < d_1 < 1$ ,  $d_2 > 1$ ,  $v_{m,j}$  and  $k_{m,j}$ ,  $j = 1, \dots, n_m$  are positive design parameters.

Define the compensation tracking errors as follows:

$$v_{m,b} = s_{m,b} - \xi_{m,b}, \quad b = 1, \dots, n_m - 1, \quad (3.7)$$

$$v_{m,n_m} = s_{m,n_m} - \xi_{m,n_m} - \psi_m, \quad (3.8)$$

where  $\psi_m$  is the saturation compensation signal, which is designed as

$$\dot{\psi}_m = -\psi_m^{d_1} - \psi_m^{d_2} + \iota_m(\varphi_m) - \varphi_m.$$

**Remark 2.** Different from asymptotically convergent saturation compensation systems [22, 23], fractional power terms  $-\psi_m^{d_1} - \psi_m^{d_2}$  are constructed to ensure that the compensation system converges within a fixed time.

Design the distributed virtual control signal  $\alpha_{m,b}$  and the fixed-time distributed controller  $\varphi_m$  as follows:

$$\alpha_{m,1} = \frac{1}{(\ell_m + J_m)} \left( -v_{m,1}v_{m,1}^{4d_1-3} - k_{m,1}v_{m,1}^{4d_2-3} - \frac{1}{2a_{m,1}^2} v_{m,1}^3 \hat{\theta}_{m,1} S_{m,1}^\top S_{m,1} + \sum_{l \in \mathfrak{N}_m} c_{m,l} x_{l,2} + \ell_m \dot{r} \right) - \frac{3}{4} v_{m,1}, \quad (3.9)$$

$$\alpha_{m,2} = -v_{m,2}v_{m,2}^{4d_1-3} - k_{m,2}v_{m,2}^{4d_2-3} - \frac{1}{2a_{m,2}^2} v_{m,2}^3 \hat{\theta}_{m,2} S_{m,2}^\top S_{m,2} - \left( \frac{1}{4} (\ell_m + J_m) + \frac{3}{4} \right) v_{m,2} + \dot{\pi}_{m,2}, \quad (3.10)$$

$$\alpha_{m,b} = -v_{m,b}v_{m,b}^{4d_1-3} - k_{m,b}v_{m,b}^{4d_2-3} - \frac{1}{2a_{m,b}^2} v_{m,b}^3 \hat{\theta}_{m,b} S_{m,b}^\top S_{m,b} + \dot{\pi}_{m,b} - v_{m,b}, \quad (3.11)$$

$$\varphi_m = -v_{m,n_m}v_{m,n_m}^{4d_1-3} - k_{m,n_m}v_{m,n_m}^{4d_2-3} - \frac{1}{2a_{m,n_m}^2} v_{m,n_m}^3 \hat{\theta}_{m,n_m} S_{m,n_m}^\top S_{m,n_m} + \dot{\pi}_{m,n_m} - v_{m,n_m} - \psi_m^{d_1} - \psi_m^{d_2}, \quad (3.12)$$

where  $b = 3, \dots, n_m - 1$ . The adaptive law  $\hat{\theta}_{m,b}$  is designed as

$$\dot{\hat{\theta}}_{m,b} = \frac{\lambda_{m,b}}{2a_{m,b}^2} v_{m,b}^6 S_{m,b}^\top S_{m,b} - \gamma_{m,b} \hat{\theta}_{m,b}, \quad b = 1, \dots, n_m, \quad (3.13)$$

where  $a_{m,b}$ ,  $\gamma_{m,b}$  and  $\lambda_{m,b}$  are positive design parameters.

#### 4. Stability analysis

**Theorem 1.** For non-triangular SNMASs with input saturation satisfying Assumptions 1 and 2, the error compensation signals (3.4)–(3.6), the virtual control signals (3.9)–(3.11), the designed distributed controller (3.12), and the adaptive law (3.13) ensure that all signals in the closed-loop system are fixed-time bounded in probability, and the consensus error between followers and the leader converges to a sufficiently small neighborhood of the origin in probability within a fixed time.

*Proof.* The detailed proof is presented as follows:

*Step 1.* From (2.2), (3.1) and (3.7), one has

$$\begin{aligned} dv_{m,1} = & \left( (\ell_m + J_m) (v_{m,2} + \xi_{m,2} + \pi_{m,2} + f_{m,1} - \alpha_{m,1} + \alpha_{m,1}) - \ell_m \dot{r} - \dot{\xi}_{m,1} \right. \\ & \left. - \sum_{l \in \mathfrak{N}_m} c_{m,l} (x_{l,2} + f_{l,1}) \right) dt + \left( (\ell_m + J_m) h_{m,1} - \sum_{l \in \mathfrak{N}_m} c_{m,l} h_{l,1} \right) d\omega. \end{aligned} \quad (4.1)$$

Choose the Lyapunov function as

$$V_{m,1} = \frac{1}{4} v_{m,1}^4 + \frac{1}{4} \xi_{m,1}^4 + \frac{1}{2\lambda_{m,1}} \tilde{\theta}_{m,1}^2.$$

According to Definition 1,  $\mathcal{L}V_{m,1}$  is computed as

$$\begin{aligned} \mathcal{L}V_{m,1} = & v_{m,1}^3 \left( (\ell_m + J_m) (v_{m,2} + \xi_{m,2} + \pi_{m,2} + f_{m,1} - \alpha_{m,1} + \alpha_{m,1}) - \ell_m \dot{r} - \dot{\xi}_{m,1} \right. \\ & \left. - \sum_{l \in \mathfrak{N}_m} c_{m,l} (x_{l,2} + f_{l,1}) \right) + \xi_{m,1}^3 \dot{\xi}_{m,1} - \frac{1}{\lambda_{m,1}} \tilde{\theta}_{m,1} \dot{\tilde{\theta}}_{m,1} \\ & + \frac{3}{2} v_{m,1}^2 \left( (\ell_m + J_m) h_{m,1} - \sum_{l \in \mathfrak{N}_m} c_{m,l} h_{l,1} \right)^\top \left( (\ell_m + J_m) h_{m,1} - \sum_{l \in \mathfrak{N}_m} c_{m,l} h_{l,1} \right). \end{aligned} \quad (4.2)$$

By utilizing Lemma 2, one yields

$$\begin{aligned} & \frac{3}{2} v_{m,1}^2 \left( (\ell_m + J_m) h_{m,1} - \sum_{l \in \mathfrak{N}_m} c_{m,l} h_{l,1} \right)^\top \left( (\ell_m + J_m) h_{m,1} - \sum_{l \in \mathfrak{N}_m} c_{m,l} h_{l,1} \right) \\ & \leq \frac{3}{4} v_{m,1}^4 \left\| (\ell_m + J_m) h_{m,1} - \sum_{l \in \mathfrak{N}_m} c_{m,l} h_{l,1} \right\|^4 + \frac{3}{4}. \end{aligned} \quad (4.3)$$

Define

$$\bar{f}_{m,1} = (\ell_m + J_m) f_{m,1} - \sum_{l \in \mathfrak{N}_m} c_{m,l} f_{l,1} + \frac{3}{4} v_{m,1} \left\| (\ell_m + J_m) h_{m,1} - \sum_{l \in \mathfrak{N}_m} c_{m,l} h_{l,1} \right\|^4 + \frac{3}{4} v_{m,1}.$$

According to Lemma 1, a FLS being used to identify  $\bar{f}_{m,1}$ , it follows that

$$\bar{f}_{m,1} = \Phi_{m,1}^\top S_{m,1} (x_m, x_l) + \sigma_{m,1} (x_m, x_l), \quad |\sigma_{m,1} (x_m, x_l)| \leq \varepsilon_{m,1}.$$



According to the property of the FLS, one has

$$S_{m,1}^\top(x_m, x_l) S_{m,1}(x_m, x_l) \leq S_{m,1}^\top(x_{m,1}, x_{l,1}) S_{m,1}(x_{m,1}, x_{l,1}).$$

Based on Lemma 2, it can be concluded that

$$v_{m,1}^3 \bar{f}_{m,1} \leq \frac{1}{2a_{m,1}^2} v_{m,1}^6 \|\Phi_{m,1}\|^2 S_{m,1}^\top(x_{m,1}, x_{l,1}) S_{m,1}(x_{m,1}, x_{l,1}) + \frac{1}{2} a_{m,1}^2 + \frac{3}{4} v_{m,1}^4 + \frac{1}{4} \varepsilon_{m,1}^4, \quad (4.4)$$

$$(\ell_m + J_m) v_{m,1}^3 v_{m,2} \leq (\ell_m + J_m) \left( \frac{3}{4} v_{m,1}^4 + \frac{1}{4} v_{m,2}^4 \right). \quad (4.5)$$

According to (4.2)–(4.5), the following inequality can be acquired:

$$\begin{aligned} \mathcal{L}V_{m,1} &\leq v_{m,1}^3 \left( (\ell_m + J_m) \left( \frac{3}{4} v_{m,1} + \xi_{m,2} + \pi_{m,2} - \alpha_{m,1} + \alpha_{m,1} \right) - \ell_m \dot{r} \right. \\ &\quad \left. - \sum_{l \in \mathcal{N}_m} c_{m,l} x_{l,2} - \dot{\xi}_{m,1} + \frac{1}{2a_{m,1}^2} v_{m,1}^3 \theta_{m,1} S_{m,1}^\top S_{m,1} \right) + \frac{1}{4} (\ell_m + J_m) v_{m,2}^4 \\ &\quad - \frac{1}{\lambda_{m,1}} \tilde{\theta}_{m,1} \dot{\theta}_{m,1} + \frac{3}{4} + \frac{1}{2} a_{m,1}^2 + \frac{1}{4} \varepsilon_{m,1}^4 + \xi_{m,1}^3 \dot{\xi}_{m,1}. \end{aligned} \quad (4.6)$$

By substituting (3.4), (3.9) and (3.13) into (4.6), it yields

$$\begin{aligned} \mathcal{L}V_{m,1} &\leq -v_{m,1} v_{m,1}^{4d_1} - k_{m,1} v_{m,1}^{4d_2} + v_{m,1} \xi_{m,1}^{4d_1-3} v_{m,1}^3 + k_{m,1} \xi_{m,1}^{4d_2-3} v_{m,1}^3 \\ &\quad + \frac{\gamma_{m,1}}{\lambda_{m,1}} \tilde{\theta}_{m,1} \hat{\theta}_{m,1} + \frac{1}{4} (\ell_m + J_m) v_{m,2}^4 + \frac{1}{2} a_{m,1}^2 + \frac{1}{4} \varepsilon_{m,1}^4 + \frac{3}{4} \\ &\quad + \xi_{m,1}^3 (\ell_m + J_m) (\pi_{m,2} - \alpha_{m,1} + \xi_{m,2}) - k_{m,1} \xi_{m,1}^{4d_2} - v_{m,1} \xi_{m,1}^{4d_1}. \end{aligned} \quad (4.7)$$

Based on Lemma 2, the following inequalities are satisfied:

$$v_{m,1} \xi_{m,1}^{4d_1-3} v_{m,1}^3 \leq \frac{4d_1 - 3}{4d_1} v_{m,1} \xi_{m,1}^{4d_1} + \frac{3}{4d_1} v_{m,1} v_{m,1}^{4d_1}, \quad (4.8)$$

$$k_{m,1} \xi_{m,1}^{4d_2-3} v_{m,1}^3 \leq \frac{4d_2 - 3}{4d_2} k_{m,1} \xi_{m,1}^{4d_2} + \frac{3}{4d_2} k_{m,1} v_{m,1}^{4d_2}. \quad (4.9)$$

By substituting (4.8) and (4.9) into (4.7), it follows that

$$\begin{aligned} \mathcal{L}V_{m,1} &\leq - \left( 1 - \frac{3}{4d_1} \right) v_{m,1} v_{m,1}^{4d_1} - \frac{3}{4d_1} v_{m,1} \xi_{m,1}^{4d_1} + \frac{\gamma_{m,1}}{\lambda_{m,1}} \tilde{\theta}_{m,1} \hat{\theta}_{m,1} \\ &\quad - \left( 1 - \frac{3}{4d_2} \right) k_{m,1} v_{m,1}^{4d_2} - \frac{3}{4d_2} k_{m,1} \xi_{m,1}^{4d_2} + \frac{1}{4} (\ell_m + J_m) v_{m,2}^4 \\ &\quad + \frac{3}{4} + \frac{1}{2} a_{m,1}^2 + \frac{1}{4} \varepsilon_{m,1}^4 + \xi_{m,1}^3 (\ell_m + J_m) (\pi_{m,2} - \alpha_{m,1} + \xi_{m,2}). \end{aligned} \quad (4.10)$$

*Step b* ( $2 \leq b \leq n_m - 1$ ). Base on (2.2), (3.2) and (3.7), one has

$$dv_{m,b} = dx_{m,b} - d\xi_{m,b} - d\pi_{m,b} = (x_{m,b+1} + f_{m,b} - \dot{\pi}_{m,b} - \dot{\xi}_{m,b}) dt + h_{m,b} d\omega. \quad (4.11)$$

Choose the Lyapunov function as

$$V_{m,b} = V_{m,b-1} + \frac{1}{4}v_{m,b}^4 + \frac{1}{4}\xi_{m,b}^4 + \frac{1}{2\lambda_{m,b}}\tilde{\theta}_{m,b}^2.$$

According to Definition 1,  $\mathcal{L}V_{m,b}$  is calculated as

$$\begin{aligned} \mathcal{L}V_{m,b} = & \mathcal{L}V_{m,b-1} + v_{m,b}^3 \left( v_{m,b+1} + \xi_{m,b+1} + \pi_{m,b+1} - \alpha_{m,b} + \alpha_{m,b} - \dot{\pi}_{m,b} - \dot{\xi}_{m,b} \right) \\ & + \frac{3}{2}v_{m,b}^2 h_{m,b}^\top h_{m,b} + \xi_{m,b}^3 \dot{\xi}_{m,b} - \frac{1}{\lambda_{m,b}} \tilde{\theta}_{m,b} \dot{\hat{\theta}}_{m,b}. \end{aligned} \quad (4.12)$$

By using Lemma 2, one yields

$$\frac{3}{2}v_{m,b}^2 h_{m,b}^\top h_{m,b} \leq \frac{3}{4}v_{m,b}^4 \|h_{m,b}\|^4 + \frac{3}{4}. \quad (4.13)$$

Define

$$\bar{f}_{m,b} = f_{m,b} + \frac{3}{4}v_{m,b} \|h_{m,b}\|^4 + \frac{3}{4}v_{m,b}.$$

By applying a FLS to identify  $\bar{f}_{m,b}$ , it can be acquired that

$$\bar{f}_{m,b} = \Phi_{m,b}^\top S_{m,b}(x_m) + \sigma_{m,b}(x_m), \quad |\sigma_{m,b}(x_m)| \leq \varepsilon_{m,b}.$$

According to the property of the FLS, one has

$$S_{m,b}^\top(x_m) S_{m,b}(x_m) \leq S_{m,b}^\top(\bar{x}_{m,b}) S_{m,b}(\bar{x}_{m,b}),$$

where

$$\bar{x}_{m,b} = [x_{m,1}, \dots, x_{m,b}]^\top.$$

Based on Lemma 2, the following inequalities are satisfied:

$$v_{m,b}^3 \bar{f}_{m,b} \leq \frac{1}{2a_{m,b}^2} v_{m,b}^6 \|\Phi_{m,b}\|^2 S_{m,b}^\top(\bar{x}_{m,b}) S_{m,b}(\bar{x}_{m,b}) + \frac{1}{2}a_{m,b}^2 + \frac{3}{4}v_{m,b}^4 + \frac{1}{4}\varepsilon_{m,b}^4, \quad (4.14)$$

$$v_{m,b}^3 v_{m,b+1} \leq \frac{3}{4}v_{m,b}^4 + \frac{1}{4}v_{m,b+1}^4. \quad (4.15)$$

By utilizing (3.5), (3.10), (3.11) and (3.13), it follows that

$$\begin{aligned} \mathcal{L}V_{m,b} \leq & - \sum_{j=1}^b \left(1 - \frac{3}{4d_1}\right) v_{m,j} v_{m,j}^{4d_1} - \sum_{j=1}^b \frac{3}{4d_1} v_{m,j} \xi_{m,j}^{4d_1} - \sum_{j=1}^b \left(1 - \frac{3}{4d_2}\right) k_{m,j} v_{m,j}^{4d_2} \\ & - \sum_{j=1}^b \frac{3}{4d_2} k_{m,j} \xi_{m,j}^{4d_2} + \sum_{j=1}^b \left(\frac{3}{4} + \frac{1}{2}a_{m,j}^2 + \frac{1}{4}\varepsilon_{m,j}^4\right) + \sum_{j=1}^b \frac{\gamma_{m,j}}{\lambda_{m,j}} \tilde{\theta}_{m,j} \hat{\theta}_{m,j} \\ & + \frac{1}{4}v_{m,b+1}^4 + \sum_{j=1}^b \xi_{m,j}^3 (\ell_{m,j} + J_{m,j}) (\pi_{m,j+1} - \alpha_{m,j} + \xi_{m,j+1}). \end{aligned} \quad (4.16)$$

Step  $n_m$ . According to (2.2), (3.2) and (3.8), one has

$$\begin{aligned} dv_{m,n_m} &= \left( u_m(\varphi_m) + f_{m,n_m} - \dot{\pi}_{m,n_m} - \dot{\xi}_{m,n_m} - \dot{\psi}_m \right) dt + h_{m,n_m} d\omega \\ &= \left( \varphi_m + \bar{l}_m(\varphi_m) + \psi_m^{d_1} + \psi_m^{d_2} - \dot{\pi}_{m,n_m} - \dot{\xi}_{m,n_m} \right) dt + h_{m,n_m} d\omega. \end{aligned} \quad (4.17)$$

Choose the Lyapunov function as

$$V_{m,n_m} = V_{m,n_m-1} + \frac{1}{4}v_{m,n_m}^4 + \frac{1}{4}\xi_{m,n_m}^4 + \frac{1}{2\lambda_{m,n_m}}\tilde{\theta}_{m,n_m}^2.$$

Based on Definition 1,  $\mathcal{L}V_{m,n_m}$  is computed as

$$\begin{aligned} \mathcal{L}V_{m,n_m} &= \mathcal{L}V_{m,n_m-1} + v_{m,n_m}^3 \left( \varphi_m + \bar{l}_m(\varphi_m) + \psi_m^{d_1} + \psi_m^{d_2} - \dot{\pi}_{m,n_m} - \dot{\xi}_{m,n_m} \right) \\ &\quad + \frac{3}{2}v_{m,n_m}^2 h_{m,n_m}^\top h_{m,n_m} + \xi_{m,n_m}^3 \dot{\xi}_{m,n_m} - \frac{1}{\lambda_{m,n_m}} \tilde{\theta}_{m,n_m} \dot{\hat{\theta}}_{m,n_m}. \end{aligned} \quad (4.18)$$

By utilizing Lemma 2, the following inequalities are satisfied:

$$\frac{3}{2}v_{m,n_m}^2 h_{m,n_m}^\top h_{m,n_m} \leq \frac{3}{4}v_{m,n_m}^4 \|h_{m,n_m}\|^4 + \frac{3}{4}, \quad (4.19)$$

$$v_{m,n_m}^3 D_m \leq \frac{3}{4}v_{m,n_m}^4 + \frac{1}{4}D_m^4. \quad (4.20)$$

Define

$$\bar{f}_{m,n_m} = f_{m,n_m} + \frac{3}{4}v_{m,n_m} \|h_{m,n_m}\|^4 + \frac{3}{4}v_{m,n_m}$$

with a FLS utilized to identify  $\bar{f}_{m,n_m}$ , one yields

$$\bar{f}_{m,n_m} = \Phi_{m,n_m}^\top S_{m,n_m}(x_m) + \sigma_{m,n_m}(x_m), \quad |\sigma_{m,n_m}(x_m)| \leq \varepsilon_{m,n_m}.$$

According to Lemma 2, it can be obtained that

$$v_{m,n_m}^3 \bar{f}_{m,n_m} \leq \frac{1}{2a_{m,n_m}^2} v_{m,n_m}^6 \|\Phi_{m,n_m}\|^2 S_{m,n_m}^\top(x_m) S_{m,n_m}(x_m) + \frac{1}{2}a_{m,n_m}^2 + \frac{3}{4}v_{m,n_m}^4 + \frac{1}{4}\varepsilon_{m,n_m}^4. \quad (4.21)$$

By substituting (3.6), (3.12) and (3.13) into (4.18) and based on (4.19)–(4.21), the following inequality can be acquired:

$$\begin{aligned} \mathcal{L}V_{m,n_m} &\leq - \sum_{b=1}^{n_m} \left( 1 - \frac{3}{4d_1} \right) \gamma_{m,b} v_{m,b}^{4d_1} - \sum_{b=1}^{n_m} \frac{3}{4d_1} \gamma_{m,b} \xi_{m,b}^{4d_1} - \sum_{b=1}^{n_m} \left( 1 - \frac{3}{4d_2} \right) k_{m,b} v_{m,b}^{4d_2} \\ &\quad + \sum_{b=1}^{n_m} \left( \frac{3}{4} + \frac{1}{2}a_{m,b}^2 + \frac{1}{4}\varepsilon_{m,b}^4 \right) + \sum_{b=1}^{n_m} \frac{\gamma_{m,b}}{\lambda_{m,b}} \tilde{\theta}_{m,b} \hat{\theta}_{m,b} + \frac{1}{4}D_m^4 \\ &\quad - \sum_{b=1}^{n_m} \frac{3}{4d_2} k_{m,b} \xi_{m,b}^{4d_2} + \sum_{b=1}^{n_m-1} \xi_{m,b}^3 (\ell_{m,b} + J_{m,b}) (\pi_{m,b+1} - \alpha_{m,b} + \xi_{m,b+1}). \end{aligned} \quad (4.22)$$

By using

$$\tilde{\theta}_{m,b} = \theta_{m,b} - \hat{\theta}_{m,b},$$

and combined with Lemma 2, one has

$$\begin{aligned}\tilde{\theta}_{m,b}\hat{\theta}_{m,b} &= \tilde{\theta}_{m,b}\theta_{m,b} - \tilde{\theta}_{m,b}^2 \\ &\leq \left(\frac{1}{2}\tilde{\theta}_{m,b}^2 + \frac{1}{2}\theta_{m,b}^2\right) - \tilde{\theta}_{m,b}^2 \\ &\leq -\frac{1}{2}\tilde{\theta}_{m,b}^2 + \frac{1}{2}\theta_{m,b}^2.\end{aligned}\quad (4.23)$$

By substituting (4.23) into (4.22), one yields

$$\begin{aligned}\mathcal{L}V_{m,n_m} &\leq -\sum_{b=1}^{n_m} \left(1 - \frac{3}{4d_1}\right) v_{m,b} v_{m,b}^{4d_1} - \sum_{b=1}^{n_m} \frac{3}{4d_1} v_{m,b} \xi_{m,b}^{4d_1} - \sum_{b=1}^{n_m} \frac{\gamma_{m,b}}{2\lambda_{m,b}} \tilde{\theta}_{m,b}^2 - \sum_{b=1}^{n_m} \left(1 - \frac{3}{4d_2}\right) k_{m,b} v_{m,b}^{4d_2} \\ &\quad - \sum_{b=1}^{n_m} \frac{3}{4d_2} k_{m,b} \xi_{m,b}^{4d_2} - \sum_{b=1}^{n_m} \left(\frac{\gamma_{m,b}}{2}\right)^{d_2} \left(\frac{\tilde{\theta}_{m,b}^2}{2\lambda_{m,b}}\right)^{d_2} + \sum_{b=1}^{n_m} \left(\frac{\gamma_{m,b}}{2}\right)^{d_1} \left(\frac{\tilde{\theta}_{m,b}^2}{2\lambda_{m,b}}\right)^{d_1} - \sum_{b=1}^{n_m} \left(\frac{\gamma_{m,b}}{2}\right)^{d_1} \left(\frac{\tilde{\theta}_{m,b}^2}{2\lambda_{m,b}}\right)^{d_1} \\ &\quad + \sum_{b=1}^{n_m} \frac{\gamma_{m,b}}{2\lambda_{m,b}} \theta_{m,b}^2 + \sum_{b=1}^{n_m-1} \xi_{m,b}^3 (\ell_{m,b} + J_{m,b}) (\pi_{m,b+1} - \alpha_{m,b} + \xi_{m,b+1}) + \frac{1}{4} D_m^4 \\ &\quad + \sum_{b=1}^{n_m} \left(\frac{3}{4} + \frac{1}{2} a_{m,b}^2 + \frac{1}{4} \varepsilon_{m,b}^4\right) + \sum_{b=1}^{n_m} \left(\frac{\gamma_{m,b}}{2}\right)^{d_2} \left(\frac{\tilde{\theta}_{m,b}^2}{2\lambda_{m,b}}\right)^{d_2}.\end{aligned}\quad (4.24)$$

Based on Lemma 3, it follows that

$$\begin{aligned}\mathcal{L}V_{m,n_m} &\leq -k_{d_1} \left(\sum_{b=1}^{n_m} \frac{v_{m,b}^4}{4}\right)^{d_1} - k_{d_1} \left(\sum_{b=1}^{n_m} \frac{\xi_{m,b}^4}{4}\right)^{d_1} + \sum_{b=1}^{n_m} \frac{\gamma_{m,b}}{2\lambda_{m,b}} \theta_{m,b}^2 - \sum_{b=1}^{n_m} \frac{\gamma_{m,b}}{2\lambda_{m,b}} \tilde{\theta}_{m,b}^2 \\ &\quad - \bar{k}_{d_2} \left(\sum_{b=1}^{n_m} \frac{\xi_{m,b}^4}{4}\right)^{d_2} - k_{d_1} \left(\sum_{b=1}^{n_m} \frac{\tilde{\theta}_{m,b}^2}{2\lambda_{m,b}}\right)^{d_1} - \bar{k}_{d_2} \left(\sum_{b=1}^{n_m} \frac{v_{m,b}^4}{4}\right)^{d_2} - \bar{k}_{d_2} \left(\sum_{b=1}^{n_m} \frac{\tilde{\theta}_{m,b}^2}{2\lambda_{m,b}}\right)^{d_2} \\ &\quad + \sum_{b=1}^{n_m} \left(\frac{\gamma_{m,b}}{2}\right)^{d_1} \left(\frac{\tilde{\theta}_{m,b}^2}{2\lambda_{m,b}}\right)^{d_1} + \sum_{b=1}^{n_m-1} \xi_{m,b}^3 (\ell_{m,b} + J_{m,b}) (\pi_{m,b+1} - \alpha_{m,b} + \xi_{m,b+1}) \\ &\quad + \sum_{b=1}^{n_m} \left(\frac{3}{4} + \frac{1}{2} a_{m,b}^2 + \frac{1}{4} \varepsilon_{m,b}^4\right) + \sum_{b=1}^{n_m} \left(\frac{\gamma_{m,b}}{2}\right)^{d_2} \left(\frac{\tilde{\theta}_{m,b}^2}{2\lambda_{m,b}}\right)^{d_2} + \frac{1}{4} D_m^4,\end{aligned}\quad (4.25)$$

where

$$\begin{aligned}k_{d_1} &= \min \left\{ (1 - 3/4d_1) 4^{d_1} v_{m,b}, (3/4d_1) 4^{d_1} v_{m,b}, (\gamma_{m,b}/2)^{d_1} \right\}, \\ \bar{k}_{d_2} &= n_m^{1-d_2} \min \left\{ (1 - 3/4d_2) 4^{d_2} k_{m,b}, (3/4d_2) 4^{d_2} k_{m,b}, (\gamma_{m,b}/2)^{d_2} \right\}.\end{aligned}$$

According to Lemma 2, let  $X_1 = 1$ ,  $X_2 = \frac{\gamma_{m,b}}{4\lambda_{m,b}} \tilde{\theta}_{m,b}^2$ ,  $q_1 = 1 - d_1$ ,  $q_2 = d_1$ ,  $q_3 = d_1^{\frac{d_1}{1-d_1}}$ , and one yields

$$\sum_{b=1}^{n_m} \left(\frac{\gamma_{m,b}}{4\lambda_{m,b}} \tilde{\theta}_{m,b}^2\right)^{d_1} \leq n_m (1 - d_1) d_1^{\frac{d_1}{1-d_1}} + \sum_{b=1}^{n_m} \frac{\gamma_{m,b}}{4\lambda_{m,b}} \tilde{\theta}_{m,b}^2.\quad (4.26)$$

By substituting (4.26) into (4.25) and utilizing Lemma 3,  $\mathcal{L}V_{m,n_m}$  can be expressed as

$$\mathcal{L}V_{m,n_m} \leq -k_{d_1}V_{m,n_m}^{d_1} - k_{d_2}V_{m,n_m}^{d_2} + \sum_{b=1}^{n_m} \left( \frac{\gamma_{m,b}}{4\lambda_{m,b}} \tilde{\theta}_{m,b}^2 \right)^{d_2} - \sum_{b=1}^{n_m} \frac{\gamma_{m,b}}{4\lambda_{m,b}} \tilde{\theta}_{m,b}^2 + \hat{\Lambda}_m, \quad (4.27)$$

where

$$\begin{aligned} k_{d_2} &= 3^{1-d_2} \bar{k}_{d_2}, \\ \hat{\Lambda}_m &= \sum_{b=1}^{n_m} \left( \frac{3}{4} + \frac{1}{2} a_{m,b}^2 + \frac{1}{4} \varepsilon_{m,b}^4 \right) + \sum_{b=1}^{n_m-1} \xi_{m,b}^3 (\ell_{m,b} + J_{m,b}) (\pi_{m,b+1} - \alpha_{m,b} + \xi_{m,b+1}) \\ &\quad + \sum_{b=1}^{n_m} \frac{\gamma_{m,b}}{2\lambda_{m,b}} \theta_{m,b}^2 + \frac{1}{4} D_m^4 + n_m(1-d_1)d_1^{\frac{d_1}{1-d_1}}. \end{aligned}$$

Assume that there exists a positive constant  $\rho_{m,b}$  such that

$$|\tilde{\theta}_{m,b}| \leq \rho_{m,b}.$$

Consider the first case, if

$$|\tilde{\theta}_{m,b}| \leq 2\sqrt{\lambda_{m,b}/\gamma_{m,b}},$$

it is easily seen that

$$\sum_{b=1}^{n_m} \left( \frac{\gamma_{m,b}}{4\lambda_{m,b}} \tilde{\theta}_{m,b}^2 \right)^{d_2} - \sum_{b=1}^{n_m} \frac{\gamma_{m,b}}{4\lambda_{m,b}} \tilde{\theta}_{m,b}^2 \leq 0. \quad (4.28)$$

Therefore, one has

$$\mathcal{L}V_{m,n_m} \leq -k_{d_1}V_{m,n_m}^{d_1} - k_{d_2}V_{m,n_m}^{d_2} + \hat{\Lambda}_m.$$

For the second case, when

$$|\tilde{\theta}_{m,b}| > 2\sqrt{\lambda_{m,b}/\gamma_{m,b}},$$

it follows that

$$\sum_{b=1}^{n_m} \left( \frac{\gamma_{m,b}}{4\lambda_{m,b}} \tilde{\theta}_{m,b}^2 \right)^{d_2} - \sum_{b=1}^{n_m} \frac{\gamma_{m,b}}{4\lambda_{m,b}} \tilde{\theta}_{m,b}^2 \leq \sum_{b=1}^{n_m} \left( \frac{\gamma_{m,b}}{4\lambda_{m,b}} \rho_{m,b}^2 \right)^{d_2} - \sum_{b=1}^{n_m} \frac{\gamma_{m,b}}{4\lambda_{m,b}} \rho_{m,b}^2. \quad (4.29)$$

Consequently, (4.27) can be rewritten as

$$\mathcal{L}V_{m,n_m} \leq -k_{d_1}V_{m,n_m}^{d_1} - k_{d_2}V_{m,n_m}^{d_2} + \Lambda_m,$$

where

$$\Lambda_m = \sum_{b=1}^{n_m} \left( \frac{\gamma_{m,b}}{4\lambda_{m,b}} \rho_{m,b}^2 \right)^{d_2} - \sum_{b=1}^{n_m} \frac{\gamma_{m,b}}{4\lambda_{m,b}} \rho_{m,b}^2 + \hat{\Lambda}_m.$$

Based on the above discussion, the following result can be obtained:

$$\mathcal{L}V_{m,n_m} \leq -k_{d_1}V_{m,n_m}^{d_1} - k_{d_2}V_{m,n_m}^{d_2} + \Lambda_m, \quad (4.30)$$

where

$$\Lambda_m = \begin{cases} \hat{\Lambda}_m, & |\tilde{\theta}_{m,b}| \leq 2\sqrt{\frac{\lambda_{m,b}}{\gamma_{m,b}}}, \\ \sum_{b=1}^{n_m} \left( \frac{\gamma_{m,b}}{4\lambda_{m,b}} \rho_{m,b}^2 \right)^{d_2} - \sum_{b=1}^{n_m} \frac{\gamma_{m,b}}{4\lambda_{m,b}} \rho_{m,b}^2 + \hat{\Lambda}_m, & |\tilde{\theta}_{m,b}| > 2\sqrt{\frac{\lambda_{m,b}}{\gamma_{m,b}}}. \end{cases} \quad (4.31)$$

According to Lemma 4, all signals in the closed-loop system are fixed-time bounded in probability, and the convergence time satisfies

$$E(T_m) \leq T_{max} = \frac{1}{k_{d_1} \zeta_m (1 - d_1)} + \frac{1}{k_{d_2} \zeta_m (d_2 - 1)}.$$

Define

$$s_1 = [s_{1,1}, \dots, s_{N,1}]^T,$$

it follows that

$$\begin{aligned} E|s_1|^4 &= E|s_{1,1}^2 + \dots + s_{N,1}^2|^2 \\ &\leq 2E(s_{1,1}^4 + \dots + s_{N,1}^4) \\ &\leq 2E(v_{1,1}^4 + \xi_{1,1}^4 + \dots + v_{N,1}^4 + \xi_{N,1}^4) \\ &\leq 8EV(t) \leq 8\Xi. \end{aligned} \quad (4.32)$$

From (3.1), it can be deduced that the consensus error

$$\bar{y} = [y_1 - r, \dots, y_N - r]^T = y - (1_N \otimes r) = (\mathfrak{P}_G + \mathcal{Q}_G)^{-1} s_1,$$

where  $\otimes$  is the Kronecker product and  $1_N$  represents an  $N$ -dimensional unit column vector. According to (4.32), it yields

$$\begin{aligned} E|y - 1_N \otimes r|^4 &\leq (|\mathfrak{P}_G + \mathcal{Q}_G|^{-1})^4 E|s_1|^4 \\ &\leq 8(|\mathfrak{P}_G + \mathcal{Q}_G|^{-1})^4 \Xi. \end{aligned} \quad (4.33)$$

For any constant  $\check{\epsilon}_m > 0$ , one has

$$E|y_m(t) - r(t)|^4 < \check{\epsilon}_m, \quad \forall t > T, \quad m = 1, \dots, N. \quad (4.34)$$

Therefore, by selecting proper control parameters, the consensus error of the follower could be converged to a sufficiently small neighborhood of the origin in probability within a fixed-time.  $\square$

## 5. Simulation results

To validate the effectiveness of the fixed-time distributed control algorithm, consider the non-triangular SNMASs with the communication topology shown in Figure 1. In this topology, there is one leader denoted as ‘‘L’’ and four followers denoted as ‘‘F1–F4’’.

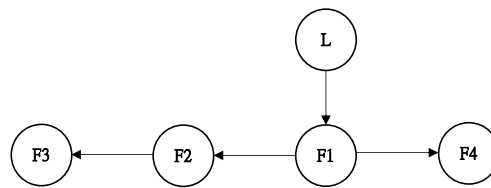


**Figure 1.** The communication topology of non-triangular SNMASs.

Consider the following non-triangular SNMASs with input saturation:

$$\begin{cases} dx_{m,1} = (x_{m,2} + f_{m,1}(x_m)) dt + h_{m,1}^\top(x_m) d\omega, \\ dx_{m,2} = (u_m(\varphi_m) + f_{m,2}(x_m)) dt + h_{m,2}^\top(x_m) d\omega, \\ y_m = x_{m,1}, \end{cases}$$

where

$$\begin{aligned} m = 1, \dots, 4, \quad x_m = [x_{m,1}, x_{m,2}]^\top, \quad f_{1,1} = x_{1,1}^4 x_{1,2}, \quad h_{1,1} = \cos(x_{1,1} x_{1,2}), \quad f_{1,2} = x_{1,1} x_{1,2}^2, \\ h_{1,2} = x_{1,1} x_{1,2}, \quad f_{2,1} = x_{2,1}^2 x_{2,2}, \quad h_{2,1} = \sin(x_{2,1} x_{2,2}), \quad f_{2,2} = x_{2,1} x_{2,2}^2, \quad h_{2,2} = x_{2,1}^3 x_{2,2}, \\ f_{3,1} = x_{3,1}^2 x_{3,2}, \quad h_{3,1} = \cos(x_{3,1}^2 x_{3,2}), \quad f_{3,2} = x_{3,1}^2 x_{3,2}, \quad h_{3,2} = x_{3,1}^3 x_{3,2}, \quad f_{4,1} = x_{4,1}^2 x_{4,2}, \\ h_{4,1} = \sin(x_{4,1} x_{4,2}), \quad f_{4,2} = x_{4,1}^2 x_{4,2}, \quad h_{4,2} = x_{4,1}^3 x_{4,2}. \end{aligned}$$

The leader's signal is given as

$$r(t) = \frac{1}{2} \sin(t) + \sin\left(\frac{1}{2}t\right).$$

The initial conditions for the followers are given as follows:

$$[x_{1,1}, x_{1,2}]^\top = [0.2, 0]^\top, \quad [x_{2,1}, x_{2,2}]^\top = [-0.6, 0]^\top, \quad [x_{3,1}, x_{3,2}]^\top = [0.7, 0]^\top, \quad [x_{4,1}, x_{4,2}]^\top = [-0.62, 0]^\top.$$

A FLS with seven fuzzy rules uniformly distributed between -3 and 3 with a width of 4 is selected. The design parameters are chosen as follows:  $d_1 = 0.8$ ,  $d_2 = 1.5$ ,  $\nu_{1,1} = 1$ ,  $k_{1,1} = 1$ ,  $\nu_{1,2} = 2$ ,  $k_{1,2} = 2$ ,  $\nu_{2,1} = 0.5$ ,  $k_{2,1} = 0.5$ ,  $\nu_{2,2} = 1$ ,  $k_{2,2} = 1$ ,  $\nu_{3,1} = 1$ ,  $k_{3,1} = 1$ ,  $\nu_{3,2} = 3$ ,  $k_{3,2} = 3$ ,  $\nu_{4,1} = 0.5$ ,  $k_{4,1} = 0.5$ ,  $\nu_{4,2} = 1$ ,  $k_{4,2} = 1$ ,  $a_{m,1} = 0.5$ ,  $a_{m,2} = 0.5$ ,  $\mathcal{B}_{m,1,1} = 14$ ,  $\mathcal{B}_{m,1,2} = 14$ ,  $\kappa_{m,1} = 10$ ,  $u_{m,\max} = 50$ ,  $u_{m,\min} = -30$ .

To demonstrate the superiority of the proposed control algorithm, a comparison is carried out with the command filter backstepping (CFB) control scheme in [12]. Define the overall tracking error

$$\text{OTE} = \sqrt{\sum_{m=1}^4 |y_m - r|^2},$$

and the root-mean-square error

$$\text{RMSE} = \sqrt{\sum_{m=1}^4 \sum_{k=1}^{\omega} (y_m(k) - r(k))^2 \omega},$$

where  $k$  is the sample index and  $\omega$  is the number of total samples. Assuming that the system's settling time is denoted by a settling time with  $\text{OTE} \leq 0.15$ .

The simulation results are shown in Figures 2–6 and Table 1. Figures 2 and 3 display the tracking curves of the followers and the curves of the consensus error  $y_m - r$  using the proposed algorithm and CFB method, respectively. Figure 4 shows the curves of the adaptive law  $\hat{\theta}_m$ . Figure 5 illustrates the curves of the designed control input  $\varphi_m$  and saturation input  $u_m(\varphi_m)$ . Figure 6 displays the OTE curves for different control schemes, and the comparison of the settling time and RMSE is presented in Table 1.

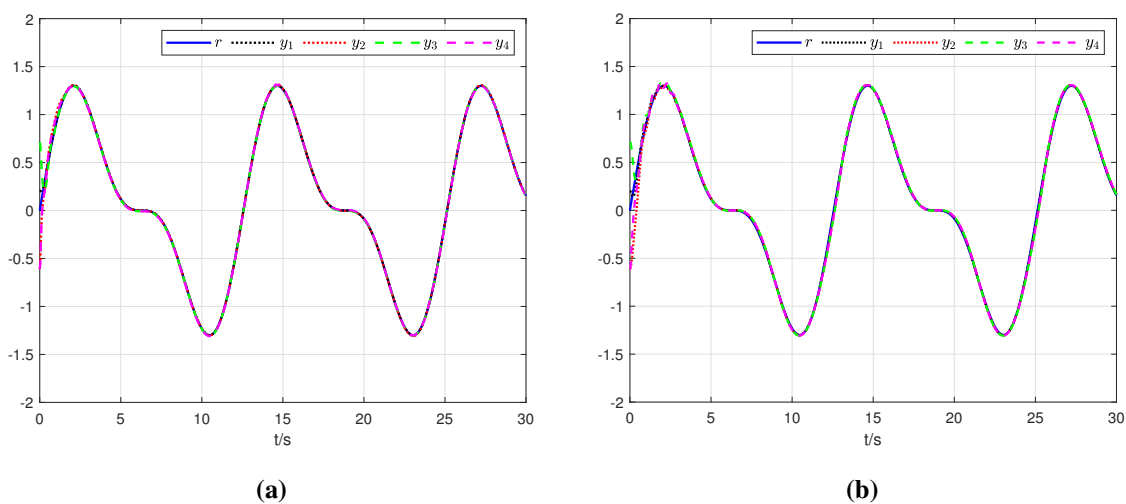


**Figure 2.** (a) Curves of follower's output signal  $y_m$  and leader's signal  $r$  (proposed). (b) Curves of follower's output signal  $y_m$  and leader's signal  $r$  (CFB).

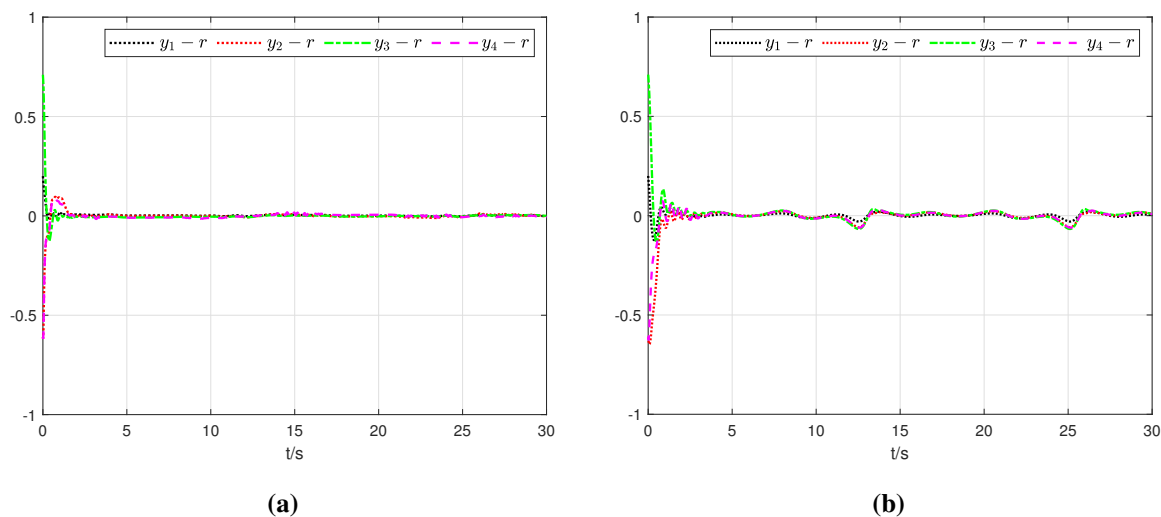


**Figure 3.** (a) Curves of consensus error  $y_m - r$  (proposed). (b) Curves of consensus error  $y_m - r$  (CFB).



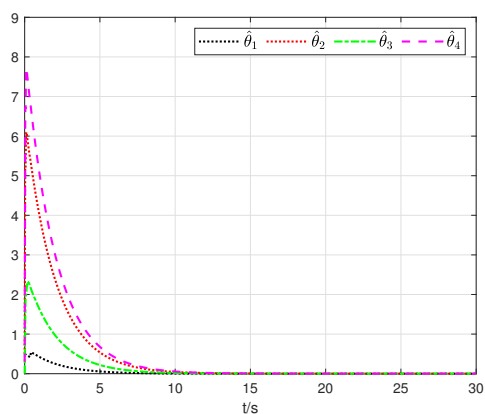


**Figure 4.** Curves of adaptation law  $\hat{\theta}_m$ .

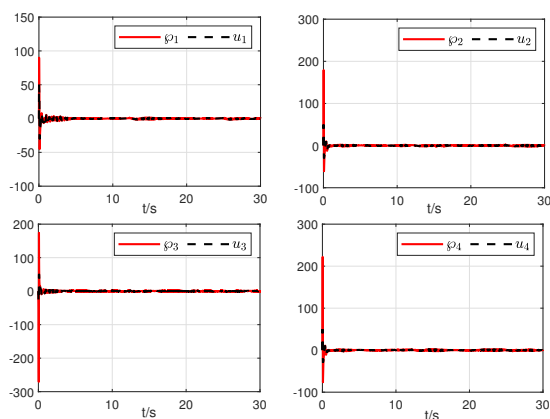


**Figure 5.** Curves of designed control input  $\varphi_m$  and saturation input  $u_m(\varphi_m)$ .

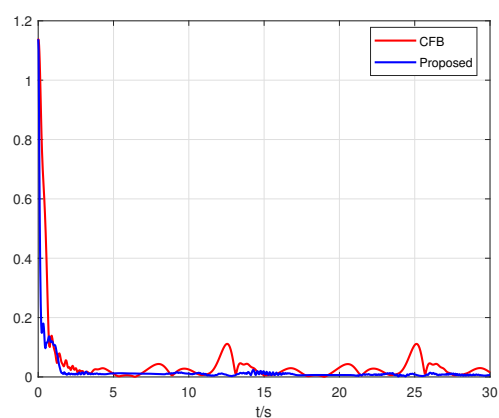


**Figure 6.** Curves of the OTE with different control schemes.

**Table 1.** Performance comparisons of settling time and RMSE.

Scheme	Settling time (s)	RMSE
Proposed	0.306	0.0475
CFB in [12]	0.965	0.2196

From the simulation results, it can be observed that all followers can precisely track the leader within 2.5 seconds, and the consensus error converges to a sufficiently small neighborhood of the origin within a fixed time. Compared to the CFB control scheme in [12], the proposed fixed-time control algorithm achieves a faster convergence rate and better consensus performance. These simulation results indicate that despite the non-triangular SNMASs being subject to input saturation and the nonlinear terms being unknown, the designed fixed-time distributed control algorithm still achieves the consensus control objective.

## 6. Conclusions

This paper has investigated the fixed-time distributed control problem for non-triangular structure SNMASs with input saturation. Based on the backstepping design method, the fixed-time command filter, and a fractional power error compensation mechanism, a fixed-time distributed consensus control algorithm has been proposed. The proposed distributed control scheme has ensured that all signals in the closed-loop system are fixed-time bounded in probability. In addition, the consensus error has converged to a sufficiently small neighborhood of the origin in probability within a fixed time. Although the proposed fixed-time distributed control algorithm achieves good consensus control, it is difficult to predetermine an expected convergence time due to the complicated relationship between the upper bound of the convergence time and various control parameters. In the future, we will focus on the predefined-time control of SNMASs on the basis of [31, 32].

### Use of AI tools declaration

The authors declare they have not used Artificial Intelligence (AI) tools in the creation of this article.

### Acknowledgments

This work was supported in part by the Natural Science Fund for Excellent Young Scholars of Jiangsu Province under Grant BK20211605 and in part by the “333 project” of Jiangsu Province.

### Conflict of interest

The authors declare no conflicts of interest.

---

## References

1. S. D. J. McArthur, E. M. Davidson, V. M. Catterson, A. L. Dimeas, N. D. Hatziargyriou, F. Ponci, et al., Multi-agent systems for power engineering applications-part I: concepts, approaches, and technical challenges, *IEEE Trans. Power Syst.*, **22** (2007), 1743–1752. <https://doi.org/10.1109/TPWRS.2007.908471>
2. Z. Pan, C. Zhang, Y. Xia, H. Xiong, X. Shao, An improved artificial potential field method for path planning and formation control of the multi-UAV systems, *IEEE Trans. Circuits Syst. II*, **69** (2022), 1129–1133. <https://doi.org/10.1109/TCSII.2021.3112787>
3. J. Zhang, J. Yan, P. Zhang, Multi-UAV formation control based on a novel back-stepping approach, *IEEE Trans. Veh. Technol.*, **69** (2020), 2437–2448. <https://doi.org/10.1109/TVT.2020.2964847>
4. Y. Yang, C. Hua, X. Guan, Multi-manipulators coordination for bilateral teleoperation system using fixed-time control approach, *Int. J. Robust Nonlinear Control*, **28** (2018), 5667–5687. <https://doi.org/10.1002/rnc.4336>
5. J. Wu, S. Qiu, M. Liu, H. Li, Y. Liu, Finite-time velocity-free relative position coordinated control of spacecraft formation with dynamic event triggered transmission, *Math. Biosci. Eng.*, **19** (2022), 6883–6906. <https://doi.org/10.3934/mbe.2022324>
6. K. Sun, H. Yu, X. Xia, Distributed control of nonlinear stochastic multi-agent systems with external disturbance and time-delay via event-triggered strategy, *Neurocomputing*, **452** (2021), 275–283. <https://doi.org/10.1016/j.neucom.2021.04.100>
7. W. Zou, C. K. Ahn, Z. Xiang, Event-triggered consensus tracking control of stochastic nonlinear multiagent systems, *IEEE Syst. J.*, **13** (2019), 4051–4059. <https://doi.org/10.1109/JSYST.2019.2910723>
8. K. Li, Y. Li, Adaptive NN optimal consensus fault-tolerant control for stochastic nonlinear multiagent systems, *IEEE Trans. Neural Netw. Learn. Syst.*, **34** (2021), 947–957. <https://doi.org/10.1109/TNNLS.2021.3104839>
9. Y. Yang, S. Miao, D. Yue, C. Xu, D. Ye, Adaptive neural containment seeking of stochastic nonlinear strict-feedback multi-agent systems, *Neurocomputing*, **400** (2020), 393–400. <https://doi.org/10.1016/j.neucom.2019.03.091>
10. X. Guo, H. Liang, Y. Pan, Observer-based adaptive fuzzy tracking control for stochastic nonlinear multi-agent systems with dead-zone input, *Appl. Math. Comput.*, **379** (2020), 125269. <https://doi.org/10.1016/j.amc.2020.125269>
11. Y. Yang, X. Xi, S. Miao, J. Wu, Event-triggered output feedback containment control for a class of stochastic nonlinear multi-agent systems, *Appl. Math. Comput.*, **418** (2022), 126817. <https://doi.org/10.1016/j.amc.2021.126817>
12. M. Shahvali, J. Askari, Distributed containment output-feedback control for a general class of stochastic nonlinear multi-agent systems, *Neurocomputing*, **179** (2016), 202–210. <https://doi.org/10.1016/j.neucom.2015.12.014>

13. Q. Wang, C. Gao, Y. Cui, L. B. Wu, Observer-based adaptive fuzzy command filtered backstepping control for stochastic nonlinear systems with event-triggered mechanism, *Int. J. Fuzzy Syst.*, **25** (2023), 1612–1623. <https://doi.org/10.1007/s40815-023-01462-9>
14. Y. Zhu, B. Niu, Z. Shang, Z. Wang, H. Wang, Distributed adaptive asymptotic consensus tracking control for stochastic nonlinear MASs with unknown control gains and output constraints, *IEEE Trans. Autom. Sci. Eng.*, 2024. <https://doi.org/10.1109/TASE.2024.3350547>
15. Y. Wu, Y. Pan, M. Chen, H. Li, Quantized adaptive finite-time bipartite NN tracking control for stochastic multiagent systems, *IEEE Trans. Cybern.*, **51** (2021), 2870–2881. <https://doi.org/10.1109/TCYB.2020.3008020>
16. X. Wang, W. Guang, T. Huang, J. Kurths, Optimized adaptive finite-time consensus control for stochastic nonlinear multiagent systems with non-affine nonlinear faults, *IEEE Trans. Autom. Sci. Eng.*, 2023. <https://doi.org/10.1109/TASE.2023.3306101>
17. A. Polyakov, Nonlinear feedback design for fixed-time stabilization of linear control systems, *IEEE Trans. Autom. Control*, **57** (2011), 2106–2110. <https://doi.org/10.1109/TAC.2011.2179869>
18. B. Cui, L. Mao, Y. Xia, T. Ma, H. Gao, Fixed-time fault-tolerant consensus control for high-order nonlinear multi-agent systems under directed topology, *IEEE Trans. Control Netw. Syst.*, **11** (2024), 197–209. <https://doi.org/10.1109/TCNS.2023.3274700>
19. X. Guo, H. Ma, H. Liang, H. Zhang, Command-filter-based fixed-time bipartite containment control for a class of stochastic multiagent systems, *IEEE Trans. Syst. Man Cybern. Syst.*, **52** (2021), 3519–3529. <https://doi.org/10.1109/TSMC.2021.3072650>
20. X. Yu, G. Wang, L. Jia, H. Zhang, Event-triggered practical fixed-time containment control for stochastic multi-agent systems with input delay, *IEEE Trans. Fuzzy Syst.*, 2024. <https://doi.org/10.1109/TFUZZ.2024.3357716>
21. Y. Zhao, H. Yu, X. Xia, Event-triggered adaptive consensus for stochastic multi-agent systems with saturated input and partial state constraints, *Inf. Sci.*, **603** (2022), 16–41. <https://doi.org/10.1016/j.ins.2022.04.035>
22. X. Song, L. Zhao, Adaptive fuzzy finite-time consensus tracking for high-order stochastic multi-agent systems with input saturation, *Int. J. Fuzzy Syst.*, **24** (2022), 3781–3795. <https://doi.org/10.1007/s40815-022-01368-y>
23. X. Yue, H. Zhang, J. Sun, L. Zhang, Distributed saturation-tolerant fuzzy control for constrained stochastic multi-agent systems with resilient quantitative behaviors, *IEEE Trans. Fuzzy Syst.*, 2024. <https://doi.org/10.1109/TFUZZ.2023.3347581>
24. S. Cheng, Z. Cheng, H. Ren, R. Lu, Adaptive fault-tolerant containment control for stochastic nonlinear multi-agent systems with input saturation, *Optim. Control Appl. Meth.*, **44** (2023), 1491–1509. <https://doi.org/10.1002/oca.2899>
25. X. Mao, *Stochastic differential equations and applications*, Cambridge: Woodhead Publishing, 2008. <https://doi.org/10.1533/9780857099402>
26. K. T. Yu, Y. M. Li, Adaptive fuzzy control for nonlinear systems with sampled data and time-varying input delay, *AIMS Math.*, **5** (2020), 2307–2325. <https://doi.org/10.3934/math.2020153>

27. W. Yan, T. Zhao, B. Niu, X. Wang, Adaptive T-S fuzzy control for an unknown structure system with a self-adjusting control accuracy, *IEEE Trans. Autom. Sci. Eng.*, 2024. <https://doi.org/10.1109/TASE.2024.3356752>
28. C. Qian, W. Lin, A continuous feedback approach to global strong stabilization of nonlinear systems, *IEEE Trans. Autom. Control*, **46** (2001), 1061–1079. <https://doi.org/10.1109/9.935058>
29. L. Zhang, B. Chen, C. Lin, Y. Shang, Fuzzy adaptive fixed-time consensus tracking control of high-order multiagent systems, *IEEE Trans. Fuzzy Syst.*, **30** (2020), 567–578. <https://doi.org/10.1109/TFUZZ.2020.3042239>
30. D. Yao, C. Dou, D. Yue, X. Xie, Event-triggered practical fixed-time fuzzy containment control for stochastic multiagent systems, *IEEE Trans. Fuzzy Syst.*, **30** (2022), 3052–3062. <https://doi.org/10.1109/TFUZZ.2021.3100930>
31. Y. Pan, C. Chen, Y. Yue, H. Liang, Event-triggered predefined-time control for full-state constrained nonlinear systems: a novel command filtering error compensation method, *Sci. China Technol. Sci.*, 2024. <https://doi.org/10.1007/s11431-023-2607-8>
32. S. Yang, Y. Pan, L. Cao, L. Chen, Predefined-time fault-tolerant consensus tracking control for Multi-UAV systems with prescribed performance and attitude constraints, *IEEE Trans. Aerosp. Electron. Syst.*, 2024. <https://doi.org/10.1109/TAES.2024.3371406>



AIMS Press

©2024 the Author(s), licensee AIMS Press. This is an open access article distributed under the terms of the Creative Commons Attribution License (<https://creativecommons.org/licenses/by/4.0>)